Expanded View Figures

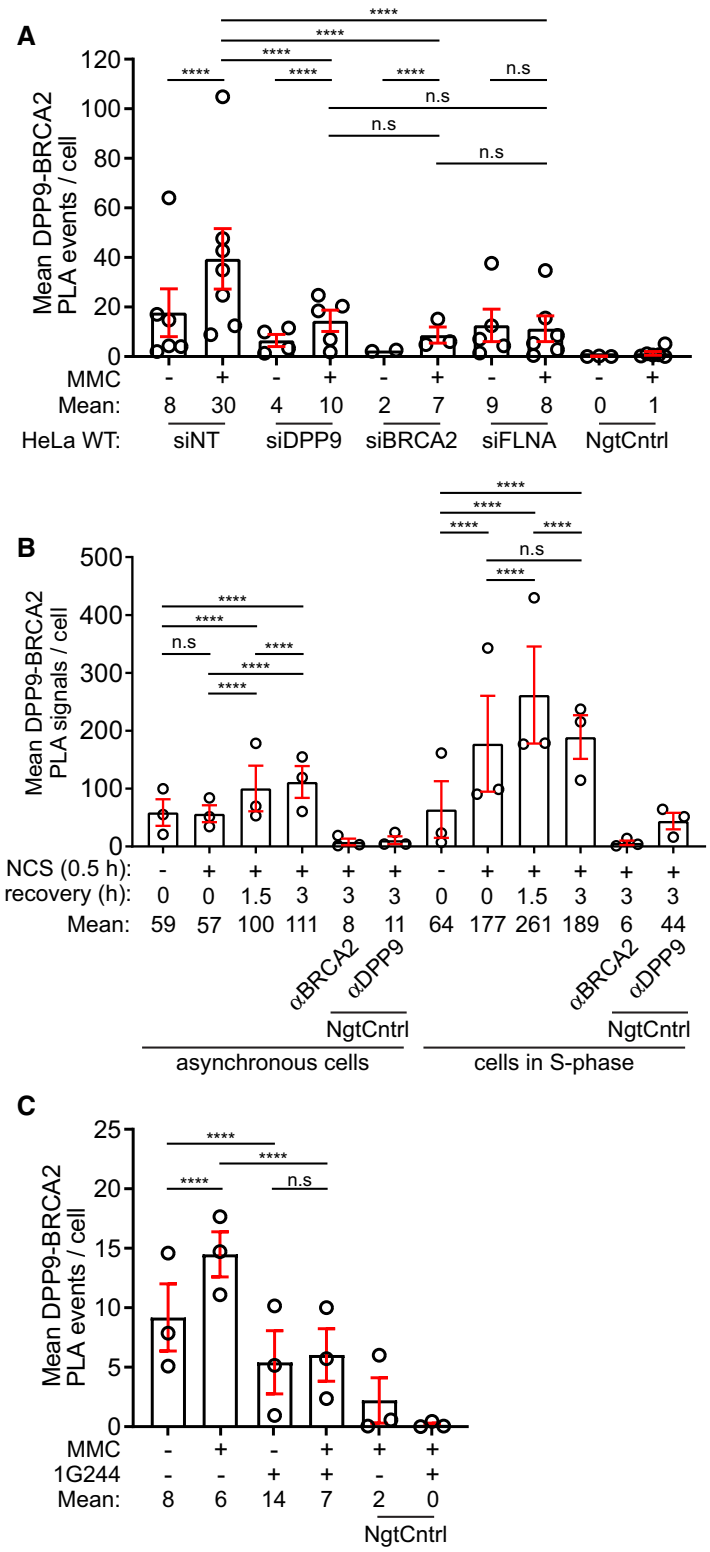

Figure EV1. Summaries of PLA experiments.

A Summary of PLAs between BRCA2 and DPP9 in control HeLa WT cells treated with nontargeting siRNA (siNT) or silenced with the indicated oligos (Fig 1B). Each dot represents the mean number of PLA events in a single repetition, from two to seven biological replicates. More than 100 cells were quantified per condition in each experiment. Data from the summary of all PLA events per cell were analyzed by a two-way ANOVA, with the Tukey's multiple comparison test. Shown are mean ± SEM (***$P \leq 0.001$, ****$P \leq 0.0001$).

B Summary of PLAs between BRCA2 and DPP9 in asynchronous HeLa WT cells and HeLa WT cells synchronized to S-phase. DNA damage was induced by NCS (250 ng/ml for 30 min). Each dot represents the mean number of PLA events in a single repetition. More than 100 cells were quantified per condition in each experiment, from three biological replicates. Data from the summary of all PLA events per cell were analyzed by a two-way ANOVA, with the Tukey's multiple comparison test. Shown are mean ± SEM (****$P \leq 0.0001$).

C Summary of PLAs between BRCA2 and DPP9 in HeLa WT cells treated with 1G244 (Fig 2C). DNA damage was induced by MMC (300 ng/ml for 24 h). Each dot represents the mean number of PLA events in a single repetition, from three biological replicates. More than 100 cells were quantified per condition in each experiment. Data from the summary of all PLA events per cell were analyzed by a two-way ANOVA, with the Tukey's multiple comparison test. Shown are mean ± SEM (****$P \leq 0.0001$).

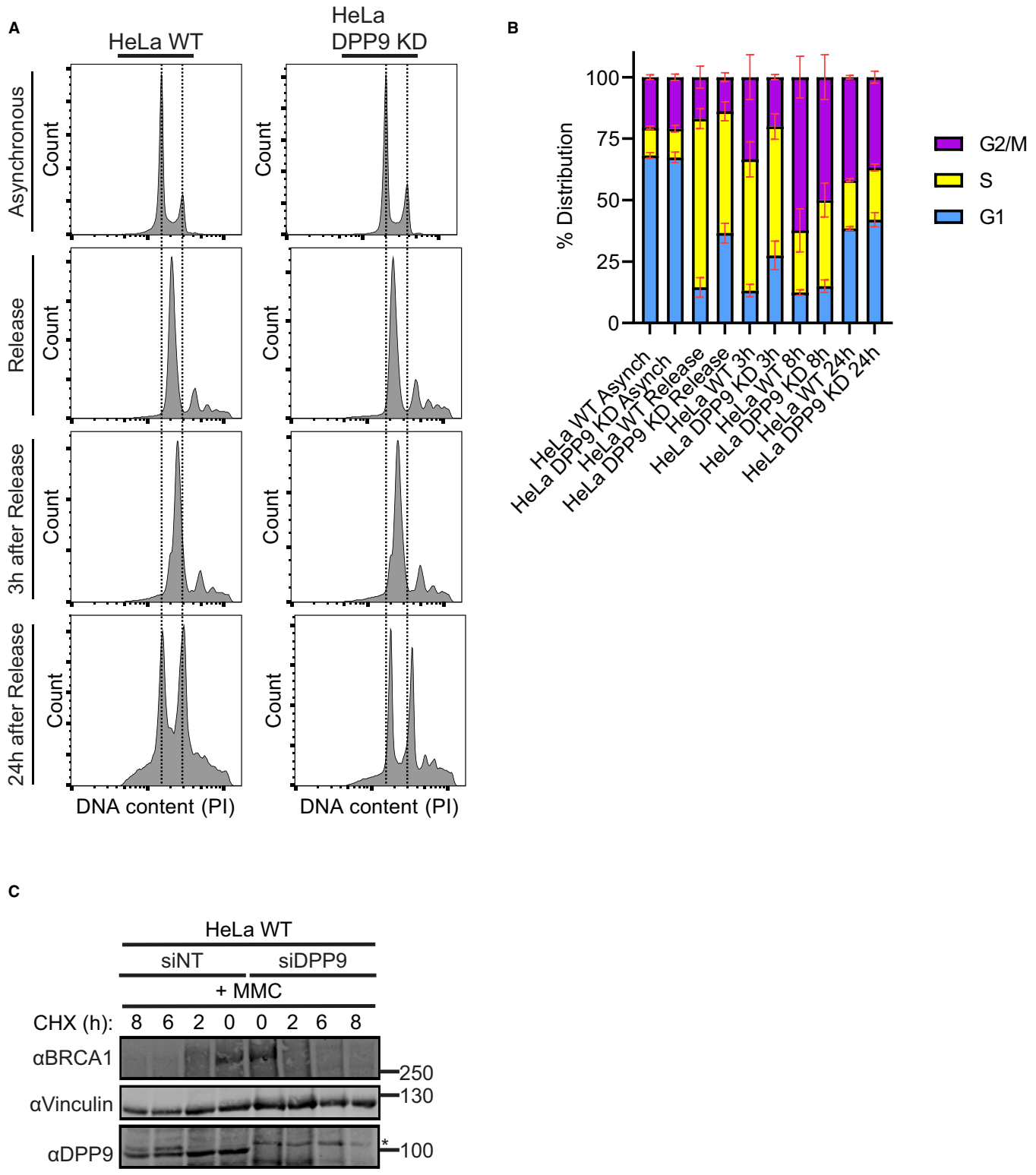
A
HeLa WT
HeLa DPP9 KD
Asynchronous
Release
3h after Release
24h after Release
Count
DNA content (PI)
B
% Distribution
100
75
50
25
0
G2/M
S
G1
HeLa WT Asynch
HeLa DPP9 KD Asynch
HeLa WT Release
HeLa DPP9 KD Release
HeLa WT 3h
HeLa DPP9 KD 3h
HeLa WT 8h
HeLa DPP9 KD 8h
HeLa WT 24h
HeLa DPP9 KD 24h
C
HeLa WT
siNT
siDPP9
+ MMC
CHX (h): 8 6 2 0 0 2 6 8
αBRCA1
αVinculin
αDPP9
250
130
100
*

Figure EV2.

Figure EV2. Characterization of DPP9-depleted HeLa cells.

A Representative histograms of HeLa WT and HeLa DPP9 KD cells investigating their relative DNA content via PI staining. Asynchronized cells and cells that were double thymidine-treated were investigated. Shown are representatives of the asynchronized, double thymidine release, 3 h of recovery and 24 h of recovery samples.

B Cell cycle distribution of the HeLa WT and HeLa DPP9 KD populations of asynchronized cells and synchronized cells at 0 h, 3, 8, and 24 after double thymidine release. Data from three to six biological replicates (asynchronized ($n = 3$), synchronized HeLa WT ($n = 6$), synchronized HeLa DPP9 KD ($n = 4$)) were analyzed by a two-way ANOVA, with the Tukey's multiple comparison test. No significant differences could be detected between the two cell lines. Shown are mean ± SEM.

C Representative western blots showing a CHX chase of HeLa WT cells transiently silenced for DPP9, and of control cells treated with nontargeting siRNA (siNT). Cells were treated with MMC (300 nM, 24 h) prior to the addition of CHX. Anti-BRCA1: RRID:AB_626761, anti-DPP9: RRID:AB_731947, anti-Vinculin: RRID:AB_477629.

Source data are available online for this figure.

Figure EV3. DPP9-deprived cells accumulate more γH2AX.

A Increased γH2AX signals in HeLa DPP9 KD cells following exposure to 300 nM MMC for 24 h. Tubulin was a loading control. Quantification of the γH2AX / Tubulin signals in HeLa DPP9 KD cells and HeLa WT cells from three biological replicates. The γH2AX / Tubulin ratio in HeLa DPP9 KD cells at 24 h MMC was defined as 100%. Mean ± SEM. Data were analyzed by a two-way ANOVA, with the Tukey's multiple comparison test (****$P \leq 0.0001$). Anti-γH2AX: RRID:AB_2118009, anti-Tubulin: RRID:AB_628412.

B Representative immunofluorescence images showing more γH2AX (white) in HeLa DPP9 KD cells following removal of Neocarzinostatin (NCS). Nuclei are shown in blue (DAPI). Scale bar 10 μm. HeLa DPP9 KD cells and HeLa WT cells were treated with 250 ng/ml Neocarzinostatin (NCS) for 30 min and allowed to recover for the indicated time points. γH2AX signals of each cell type at time 0, reflect 30 min of NCS, and no recovery time. Anti-γH2AX: RRID:AB_309864.

C Quantification of mean γH2AX signals from HeLa WT and HeLa DPP9 KD cells. More than 1,300 cells were quantified per condition per experiment. Mean ± SEM from four biological replicates, each in technical duplicates. Data were analyzed by an unpaired two-way ANOVA with the Sidak's multiple comparison test (**$P \leq 0.01$, ****$P \leq 0.0001$).

D Higher γH2AX signals in gki MEF DPP9^{S729A} cells expressing enzymatically inactive DPP9 compared with MEF WT control cells following exposure to 300 nM MMC for 24 h. Tubulin was a loading control. Quantification of the γH2AX / Tubulin ratios in gki MEF DPP9^{S729A} cells and MEF WT cells from three biological replicates. For normalization, the γH2AX / Tubulin ratio in gki MEF DPP9^{S729A} cells at 24 h MMC was defined as 100%. Mean ± SEM. Data were analyzed by a two-way ANOVA, with the Tukey's multiple comparison test (****$P \leq 0.0001$).

E Same as (C) for gki MEF DPP9^{S729A} cells and MEF WT cells. Signals from more than 1,700 cells were quantified per condition per experiment. Mean ± SEM from six biological replicates. Data were analyzed by an unpaired two-way ANOVA with the Sidak's multiple comparison test (****$P \leq 0.0001$).

Source data are available online for this figure.

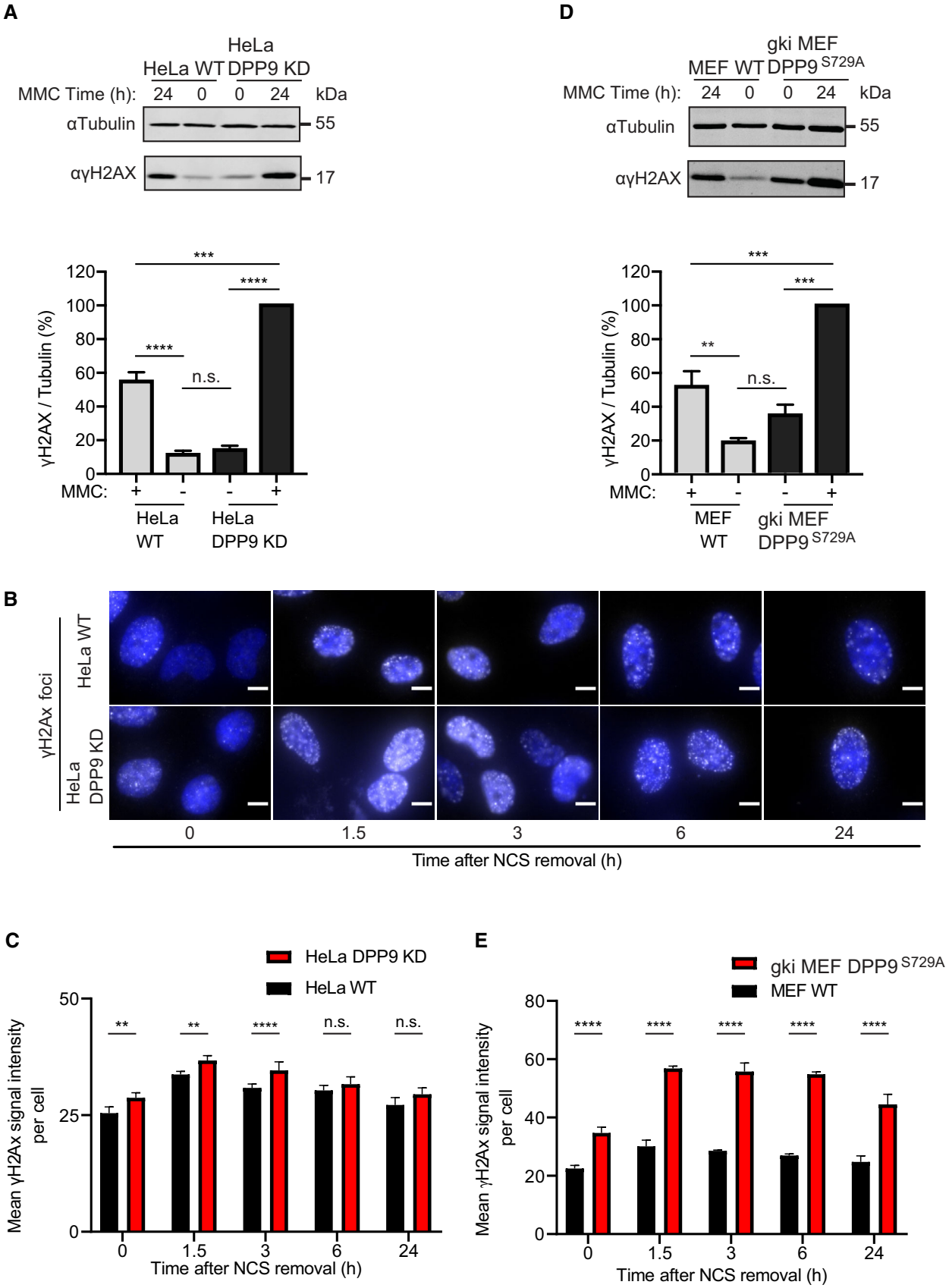
A
HeLa
HeLa WT DPP9 KD
MMC Time (h): 24 0 0 24 kDa
αTubulin 55
αγH2AX 17
γH2AX / Tubulin (%)
MMC:
HeLa WT
HeLa DPP9 KD
D
gki MEF
MEF WT DPP9 S729A
MEF WT
gki MEF DPP9 S729A
B
γH2Ax foci
HeLa WT
HeLa DPP9 KD
Time after NCS removal (h)
C
HeLa DPP9 KD
HeLa WT
Mean γH2Ax signal intensity per cell
E
gki MEF DPP9 S729A
MEF WT

Figure EV3.

Figure EV4. Summary of RAD51 experiments.

A A graph summarizing the mean number of RAD51 foci in HeLa WT cells treated with nontargeting siRNA (siNT) or silenced with the indicated oligos. Each dot represents the mean number of RAD51 foci in a single repetition, from two to six biological replicates. Statistical analysis on the data is shown in Fig 6G. Shown are mean ± SEM.

B A graph summarizing the number of RAD51 foci in HeLa WT and DPP9 KD cells treated with EdU and MMC. Shown is the quantification of RAD51 foci in EdU positive cells. HeLa DPP9 KD cells display fewer RAD51 foci in comparison with their WT counterparts. Each dot represents the number of RAD51 foci in a single cell, from three biological replicates. Data were analyzed by a two-way ANOVA, with the Tukey's multiple comparison test. Shown are mean ± SEM.

C A graph summarizing the mean number of RAD51 foci in EdU positive HeLa WT and DPP9 KD cells. Each dot represents the mean number of RAD51 foci in a single repetition, from three biological replicates. Statistical analysis on the data is shown in Fig EV4B. Shown are mean ± SEM.

D A graph summarizing the number of RAD51 foci in MEF WT and gki MEF DPP9^{S729A} cells treated with MMC. Shown is the quantification of RAD51 foci. Each dot represents the number of RAD51 foci in a single cell, from three biological replicates. Data were analyzed by a two-way ANOVA, with the Tukey's multiple comparison test. Shown are mean ± SEM.

E A graph summarizing the mean number of RAD51 foci in MEF WT and gki MEF DPP9^{S729A} cells upon MMC treatment. Each dot represents the mean number of RAD51 foci in a single repetition, from three biological replicates. Statistical analysis on the data is shown in Fig EV4D. Shown are mean ± SEM.

F A graph summarizing the mean number of RAD51 foci following induction of DPP9-S^{WT} expression, compared with uninduced HEK293 DPP9 KO+DPP9^{WT} cells (-Dox). Induction of HEK293 DPP9 KO+DPP9^{S729A} for expression of DPP9-S^{S729A} did not result in more RAD51 foci. Each dot represents the mean number of RAD51 foci in a single repetition, from three biological replicates. Statistical analysis on the data is shown in Fig 7B. Shown are mean ± SEM.

G A graph summarizing the number of RAD51 foci following induction of DPP9-S^{WT} or DPP9-L^{WT} expression, compared with HEK293 DPP9^{WT} cells. The number of RAD51 foci formed by the HEK293 DPP9 KO+DPP9-S^{WT} cells was similar to the HEK293 DPP9^{WT} cells, compared with the HEK293 DPP9 KO+DPP9-L^{WT} cells. Each dot represents the mean number of RAD51 foci in a single repetition, from two biological replicates. Shown are mean ± SEM.

H, I Summary of RAD51 foci in HeLa WT and HeLa DPP9 KD cells as described in (Fig 7C and F). Each dot represents the mean number of RAD51 foci in a single repetition, from three or four biological replicates (HeLa WT (n = 3), HeLa DPP9 KD (n = 4)). Data from the summary of all RAD51 foci per nucleus upon MMC treatment, between biological replicates, were analyzed by a two-way ANOVA, with the Tukey's multiple comparison test. Shown are mean ± SEM (****$P \leq 0.0001$). Shown are mean ± SEM.

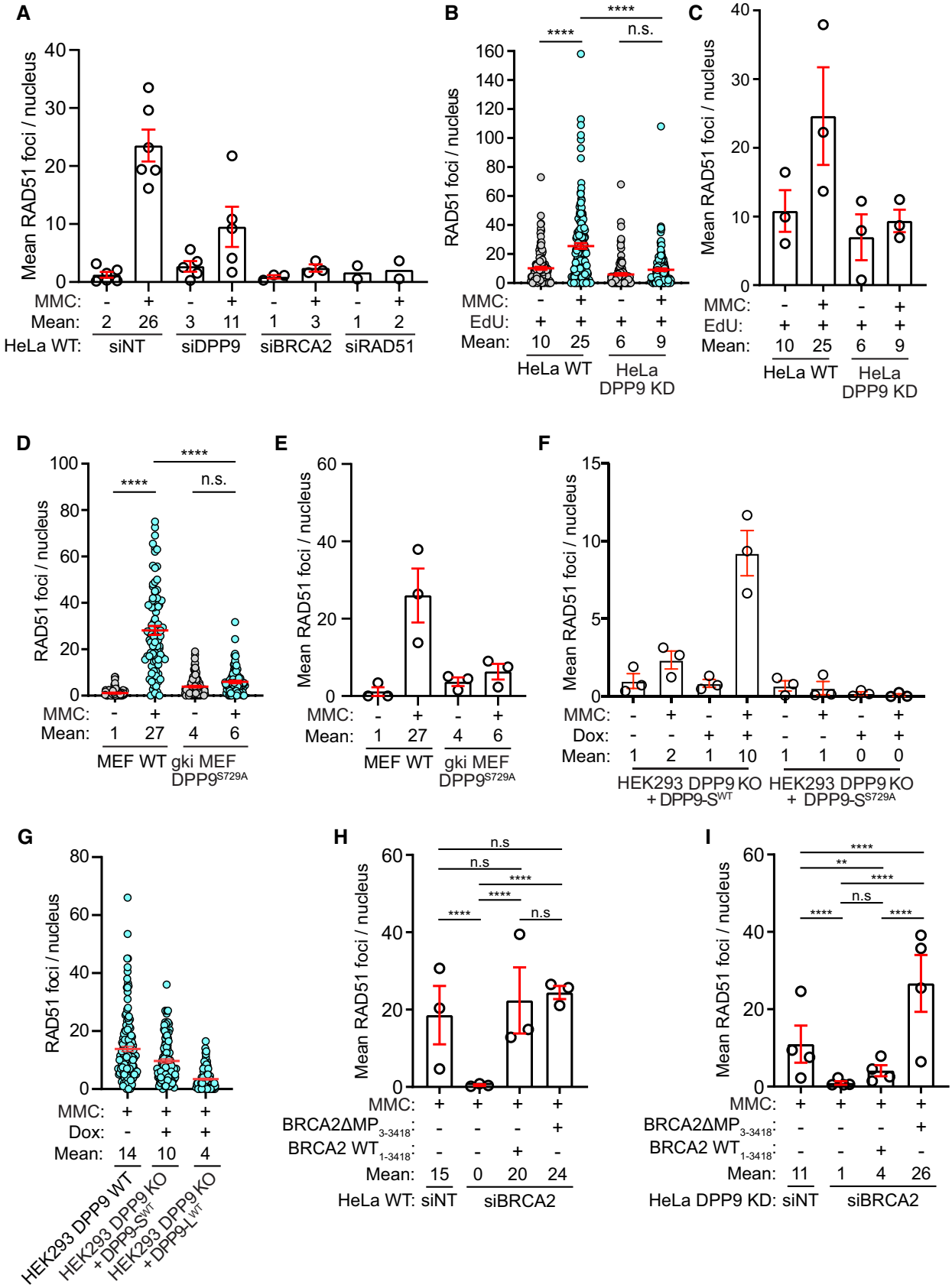
A
Mean RAD51 foci / nucleus
MMC:
Mean:
HeLa WT:
siNT
siDPP9
siBRCA2
siRAD51
B
RAD51 foci / nucleus
****
n.s.
MMC:
EdU:
Mean:
HeLa WT
HeLa DPP9 KD
C
Mean RAD51 foci / nucleus
MMC:
EdU:
Mean:
HeLa WT
HeLa DPP9 KD
D
RAD51 foci / nucleus
MMC:
Mean:
MEF WT
gki MEF DPP9S729A
E
Mean RAD51 foci / nucleus
MMC:
Mean:
MEF WT
gki MEF DPP9S729A
F
Mean RAD51 foci / nucleus
MMC:
Dox:
Mean:
HEK293 DPP9 KO + DPP9-SWT
HEK293 DPP9 KO + DPP9-S S729A
G
RAD51 foci / nucleus
MMC:
Dox:
Mean:
HEK293 DPP9 WT
HEK293 DPP9 KO + DPP9-SWT
HEK293 DPP9 KO + DPP9-LWT
H
Mean RAD51 foci / nucleus
n.s
****
MMC:
BRCA2ΔMP3-3418:
BRCA2 WT1-3418:
Mean:
HeLa WT: siNT
siBRCA2
I
Mean RAD51 foci / nucleus
**
****
n.s
MMC:
BRCA2ΔMP3-3418:
BRCA2 WT1-3418:
Mean:
HeLa DPP9 KD: siNT
siBRCA2

Figure EV4.

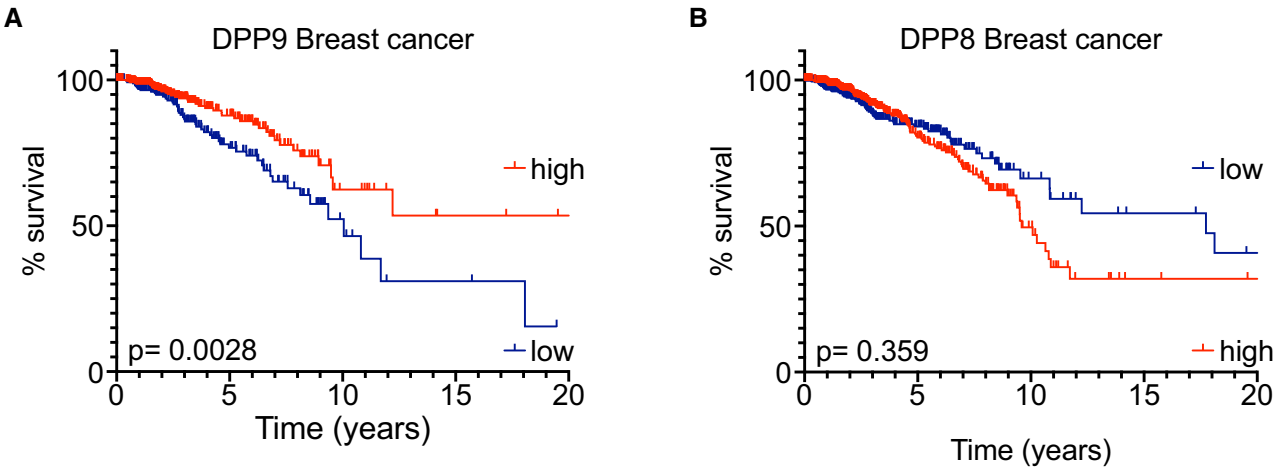

Figure EV5. Low DPP9 mRNA expression correlates with poor overall survival for patients with breast cancer.

A, B Kaplan–Meier survival curves of Breast cancer patients from The Human Protein Atlas into "high DPP9 or DPP8" (n = 282, 445) and "low DPP9 or DPP8" (n = 408, 630) mRNA expression (greater than or less than 9.678 or 4.36 reads per kilobase per million, respectively). P-values calculated by log-rank (Mantel–Cox) indicated greater overall survival in patients with high levels of DPP9 expression (A), while differences in the DPP8 levels were not statistically significant (B).